

## Synthesis and Characterization of Copper Indium Sulfide Chalcopyrite Structure with Hot Injection Method

Y. Vahidshad<sup>\*a,c</sup>, R. Ghasemzadeh<sup>a</sup>, A. Irajizad<sup>b</sup>, S. M. Mirkazemi<sup>a</sup>

<sup>a</sup> School of Metallurgy and Material Engineering, Iran University of Science and Technology, Tehran 16844, Iran.

<sup>b</sup> Department of Physics, Sharif University of Technology, Tehran 11365-9161, Iran.

<sup>c</sup> Material Research Department, Engineering research Institute, Tehran , 16844, Iran.

### Article history:

Received 3/7/2013

Accepted 22/8/2013

Published online 1/9/2013

### Keywords:

Hot injection

Chalcopyrite

Complex

Coordination Solvent

### \*Corresponding author:

E-mail address:

[yvahidshad@yahoo.com](mailto:yvahidshad@yahoo.com)

Phone: 98 912 4515282

Fax: +98 21 66282146

### Abstract

In this investigation, CuInS<sub>2</sub> ternary compound was synthesized by injection of thiourea solution into a hot copper-indium solution. The CuCl, InCl<sub>3</sub> along with (SC (NH<sub>2</sub>)<sub>2</sub>) were used as a precursor dissolved in high boiling point solvent such as oleylamine (CH(CH<sub>2</sub>)<sub>17</sub>NH<sub>2</sub>) and oleic acid (CH(CH<sub>2</sub>)<sub>16</sub>COOH) as a coordination solvent and capping agent, respectively. The size, distribution and shape were optimized by controlling some parameters such as the ratio of solvent to capping agent, anion and cation solution temperature in the instant of injection. The crystal structure, morphology, and optical properties of synthesized nanoparticles were characterized using XRD, TEM, UV-VIS-NIR and PL. The results indicate that the temperature of the solution in the instant of injection has a significant effect on the tuning of the nanocrystals size as well as narrow size distribution.

2013 JNS All rights reserved

## 1. Introduction

Copper indium sulfide (CIS) materials are known as important semiconductors that can be utilized to photovoltaic, optics, electronic and bioimaging applications. The CuInS<sub>2</sub> compound can be ideally utilized as an absorbing layer of solar cells due their high absorption coefficient ( $>10^5$  cm<sup>-1</sup>), changeable electrical conductivity (p-type to n-type), and direct band gap (1.5 eV) at near the red edge of the visible spectrum. Moreover, sulfide based composition (CuInS<sub>2</sub>) is

less toxic than selenide based compounds (CuIn(S<sub>x</sub>Se<sub>1-x</sub>)<sub>2</sub> and CuIn<sub>x</sub>Ga<sub>1-x</sub>Se<sub>2</sub>). Recent research studies mostly focus on producing CuInS<sub>2</sub> nanocolloids with uniform size and shape while their structural and optical properties are still suitable for printable optoelectronic applications [1-9]. Copper indium sulfide compound as one of the best p-type compositions has been produced with a variety of methods such as coevaporation [10, 11], sputtering [12], ion layer gas reaction [13], electro deposition [14] chemical bath

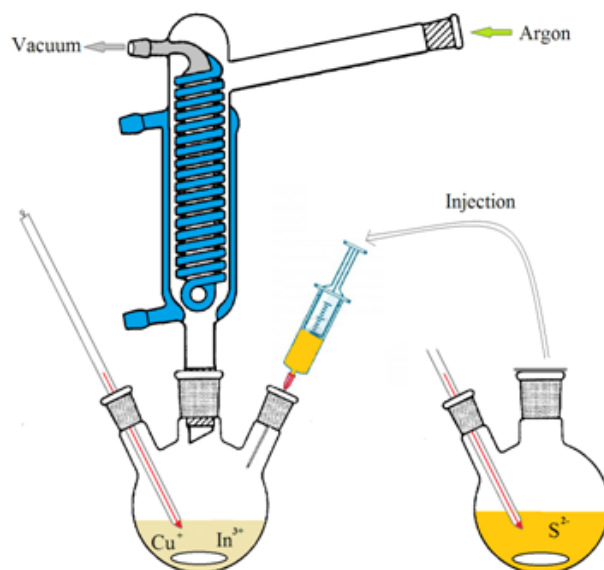
deposition [15], microwave-assisted synthesis [16], spray pyrolysis [17] and chemical wet methods for printing usage [18]. The wet chemical process is one of the best inorganic colloidal nanocrystalline producing methods due to its non-vacuum and inexpensive equipments as well as low waste of material. The hot injection synthesis as one of the wet chemical processes usually produces high quality nanocrystalline and does not require post annealing treatments. To achieve narrow size distribution appropriate coordination solvents should be exploited [19-23]. Recently, many researchers have produced the zincblende and wurtzite structures of the  $\text{CuInS}_2$  nanocrystals employing the hot injection method [24-26].

In our study, the pure chalcopyrite of  $\text{CuInS}_2$  was synthesized. Besides, the effect of coordination strength and the variety of reaction conditions on the formation and decomposition of Cu-OLA and In-OLA complex is investigated.

## 2. Experimental procedure

In this study, copper (I) chloride (99.99%, abcr), indium chloride (99.99%, abcr) and thiourea (99.99%, Sigma-Aldrich) used as a precursor. Oleylamine (OLA, 80-90%, Across) and oleic acid (OA, 90%, Fisher) used as solvent and capping agent. The  $\text{CuInS}_2$  powders were synthesized by hot injection technique. 1 mmol  $\text{CuCl}$ , 1 mmol  $\text{InCl}_3$  were dissolved into 10 ml oleylamine and 10 ml oleic acid in 100 ml three neck flask under air atmosphere then the three neck flask connected Schlenk line and stirred for at least 60 min till precursors was started to solve under vacuum. Next, the solution temperature was increased between 150-240°C under argon condition until a clear solution was obtained. At the same time 2 mmol  $\text{CH}_4\text{N}_2\text{S}$  was separately solved in 10 ml oleylamine under an argon condition with

temperature between 50-150°C. After prepared of two solutions, the thiourea solution was injected into the first solution (scheme 1).



**Scheme 1. Hot injection synthesis method for  $\text{CuInS}_2$ .**

After injection, the temperature of reaction mixture was increased to 300°C quickly (15°C/min). The reaction was held from 2 to 4 hours after which the mantle was removed and the solution was cooled down to room temperature. At room temperature around the 30 ml ethanol added to the solution for precipitating nanoparticles. The nanoparticles centrifuged for 10 min with 9000 rpm, washed several times by pure ethanol and n-hexane and finally dried at 80°C for 5 hours at air condition. The oleic acid was used as a study of capping agent. The other  $\text{CuInS}_2$  samples were synthesized by the reaction of same precursor with oleic acid and oleylamine under similar conditions. See Table 1 for details concerning solution preparation. The structural and the optical properties of the  $\text{CuInS}_2$  nanoparticles were characterized using Siemens D5000 powder diffractometer with a Braun M50 position-sensitive detector and Cu  $\text{K}\alpha 1$  radiation (Ge (220)

monochromator) with a step size of 0.039. Low-resolution TEM images were recorded on a Philips EM420 microscope operating at an acceleration voltage of 120 kV, and UV-Vis. NIR spectrophotometer (Ocean Optics In. USB-4000). The optical properties of nanoparticles are determined from absorbance measurement in the range of 300–1000 nm carried out on the toluene colloidal nanoparticles. The absorption coefficient ( $\alpha$ ) could be obtained from Beer–Lambert law:

$$\alpha = -\frac{1}{d} \ln \left( \frac{I}{I_0} \right) \Rightarrow \alpha = 2.303 \times \frac{A}{d} \quad (1)$$

**Table 1. Experimental details for hot injection method at different conditions.**

Parameters							
Solvent to capping agent ratio in metal solution			Temperature of solution 2				
Temperature of solution 1			Synthesis duration				
Sample No.	Cations Solvent Ratio	Cu:In:S	Anions Solvent	Temperature		Synthesis Temperature	Synthesis Duration
				Solution 1	Solution 2		
CIS-WOA-M1	10cc OLA + 10cc OA	(1:1:2)	20cc OLA	150°C	50°C	(10°C/min) 300°C	4 hr (100cc flask)
CIS-WOA-M2	10cc OLA + 10cc OA	(1:1:2)	20cc OLA	150°C	100°C	(10°C/min) 300°C	4 hr (100cc flask)
CIS-WOA-M3	10cc OLA + 10cc OA	(1:1:2)	20cc OLA	150°C	150°C	(10°C/min) 300°C	4 hr (100cc flask)
CIS-WOA-M4	5cc OLA + 15cc OA	(1:1:2)	20cc OLA	150°C	150°C	(10°C/min) 300°C	4 hr (100cc flask)
CIS-WOA-M5	15cc OLA + 5cc OA	(1:1:2)	20cc OLA	150°C	150°C	(10°C/min) 300°C	4 hr (100cc flask)
CIS-WOA-M6	20cc OLA + 0cc OA	(1:1:2)	20cc OLA	150°C	150°C	(10°C/min) 300°C	4 hr (100cc flask)
CIS-WOA-M7	0cc OLA + 20cc OA	(1:1:2)	20cc OLA	150°C	150°C	(10°C/min) 300°C	4 hr (100cc flask)
CIS-WOA-M8	7.5cc OLA + 2.5cc OA	(0.5:0.5:1)	10cc OLA	150°C	150°C	(16°C/min) 300°C	4 hr (100cc flask)
CIS-WOA-M9	7.5cc OLA + 2.5cc OA	(0.5:0.5:1)	10cc OLA	180°C	150°C	(18°C/min) 300°C	4 hr (100cc flask)
CIS-WOA-M10	7.5cc OLA + 2.5cc OA	(0.5:0.5:1)	10cc OLA	180°C	150°C	(18°C/min) 300°C	2 hr (100cc flask)
CIS-WOA-M11	7.5cc OLA + 2.5cc OA	(0.5:0.5:1)	10cc OLA	210°C	150°C	(18°C/min) 300°C	2 hr (100cc flask)
CIS-WOA-M12	7.5cc OLA + 2.5cc OA	(0.5:0.5:1)	10cc OLA	240°C	150°C	(19°C/min) 300°C	2 hr (100cc flask)
CIS-WOA-M13	7.5cc OLA + 2.5cc OA	(0.5:0.5:1)	10cc OLA	270°C	150°C	(20°C/min) 300°C	2 hr (100cc flask)
CIS-WOA-M14	7.5cc OLA + 2.5cc OA	(0.5:0.5:1)	10cc OLA	240°C	150°C	(19°C/min) 300°C	2 hr (250cc flask)

CIS-WOA  $\approx$  CuInS<sub>2</sub> - With Out Autoclave

### 3. Results and discussion

The possible formation mechanism of CuInS<sub>2</sub> nanocrystalline is discussed based on the experimental results. In the present experiments, Copper and indium chloride were dissolved in oleylamine and oleic acid as metal precursors. The thiourea was also dissolved in oleylamine as a sulfur source. After solving of metal salts, when the temperature increased till 100°C the formation of Cu-OLA and In-OLA complexes carried out by

Where, A is absorption of obtaining nanocrystalline from the spectrometer and d is a nanocrystalline diameter. The band gap is determined from Tauc's equation:

$$(\alpha h\nu)^n = c(h\nu - E_g) \quad (2)$$

Where, c is a constant, E<sub>g</sub> is the band gap, n is the index indicating the type of the transition. It is known that the values of n for direct, indirect, forbidden direct and indirect optical transitions are 0.5, 2, 1.5 and 3, respectively [27-30].

changing the color in the solution as shown by the proposed Equation 1 and 2. Subsequently with increasing more than 130°C, the complexes of Cu-OLA and In-OLA were decomposed to produce copper and indium ions [31-35]. In this temperature, injection of second solution including sulfur source into a copper and indium cations solution could be resulted in the nucleation of the nanocrystalline along with their growth. Narrow size distribution and small size of the particles

were obtained with control of solution temperature instant of injection as well as coordination solvent to capping agent ratio. Starting the reaction at high temperature was resulted in fast nucleation followed by slower particle growth. The obtained nanocrystalline were stabled in non-polar solvents (OLA) due to the presence of amine ( $\text{NH}_2$ ) and

carboxylic ( $\text{COOH}$ ) groups covalently connected to the particle surface. The temperature variation of solution ( $150\text{-}270^\circ\text{C}$ ) at the instant of injection was led to a change in the rate of nucleation. Accordingly, it can be inferred that temperature is really effective on the tune of the particles size and distribution.

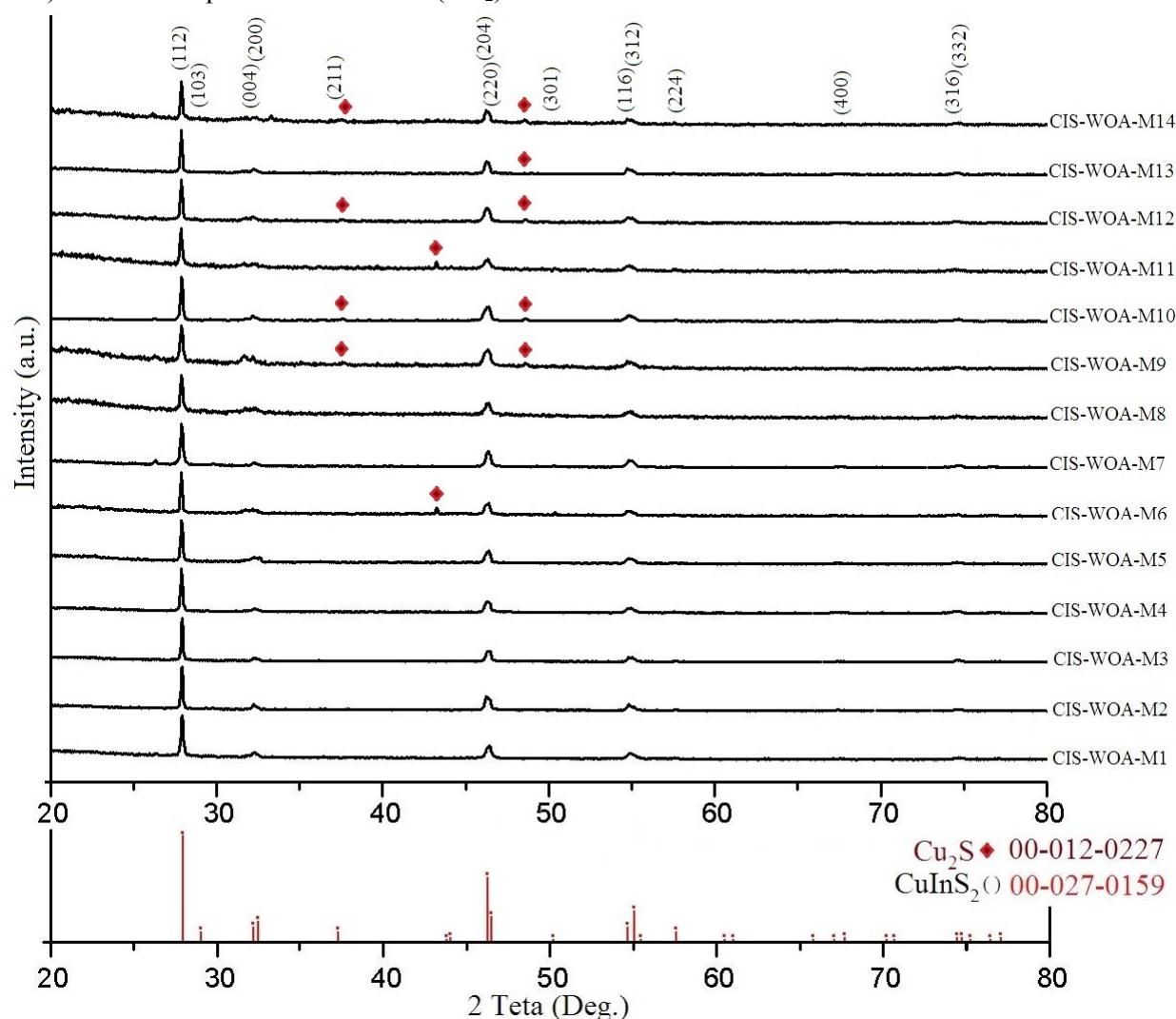
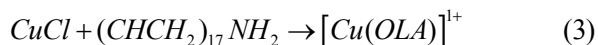


**Fig. 1.** X-ray diffraction patterns of  $\text{CuInS}_2$  samples synthesized in different conditions.

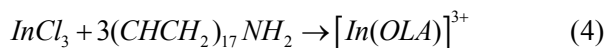
We know that the number of nuclei formation is an exponential function of temperature [36]. The injecting temperature in our synthesis was really an important parameter because when the temperature was more than  $240^\circ\text{C}$ , the synthesized particles were broadly distributed in size. It seems the

earlier nuclei that immediately formed in the near position of the injection (because of the high temperature) grew with unreacted precursors far from the injection position. However, the low temperature was resulted in slow nucleation followed by their growth as a result of reaction

with remained precursors. As a result the big particles were produced. So, the optimized temperature along with the ratio of coordination solvent to capping agent could be noticeable to achieve nano size and narrow size distribution. As the temperature of a metals solution increases, the color of the solution changed due to the formation of different complexes. Firstly, the color was blue up to 100°C due to the formation of copper complex [37]:



The color changed to between dark blue and dark green when the temperature exceeded 100°C. After 115°C, the color changed to light green because of the formation of indium complex [38]:

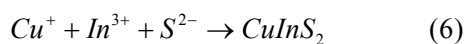


After 130°C the color changed to transparent light green because both of the complexes were completely formed. At about 200°C the smoke

began to evolve and the color turned from transparent to nontransparent up to 240°C indicating the complexes were decomposed completely followed by the nucleation of nanocrystals. In the second flask, by solving thiourea the color of solution turned to orange [39]:

$$2SC(NH_2)_2 + 2(CHCH_2)_{17}NH_2 \rightarrow S^{2-} + 2CH_4 + 2N_2 + 2(CHCH_2)_{17}NH_2 \quad (5)$$

The temperature of 240°C was the best one for injection of anion solution and formation of copper indium sulfide compound:



The extra oleylamine, oleic acid and thiourea play the role of capping agent via reacting amine (NH<sub>2</sub>) and carboxylic (COOH) ligands with nanoparticles surface. This reaction results in a slow growth process providing control of crystalline size, stabilization of colloids as well as decrease of aggregation.

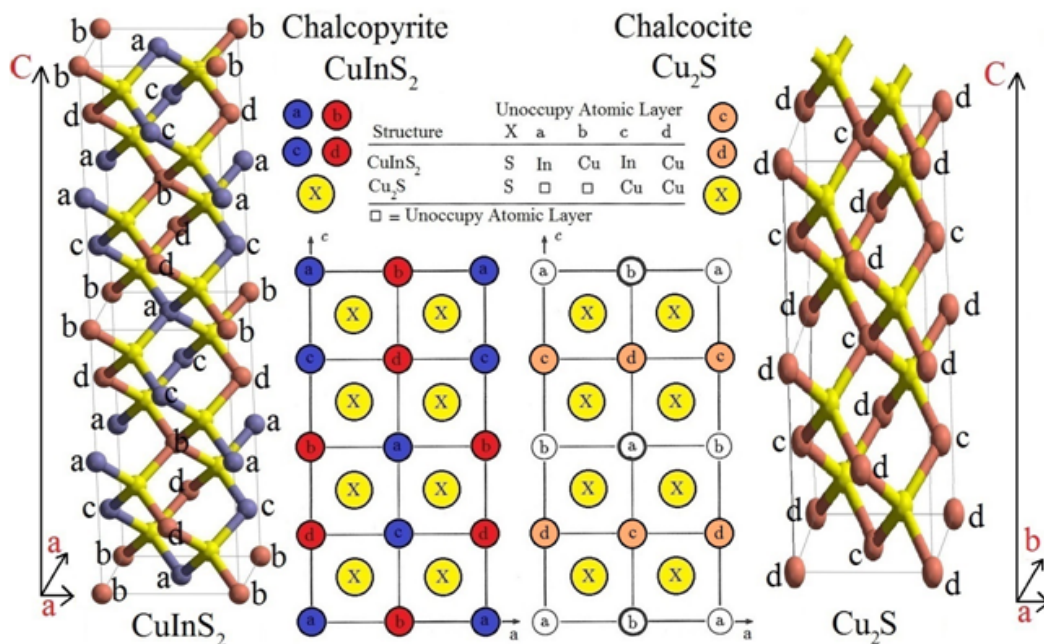


Fig. 2. The atomic positions arrangements in structure crystal of CuInS<sub>2</sub> and Cu<sub>2</sub>S.

Fig. 1. shows the XRD patterns of the synthesized CuInS<sub>2</sub> nanocrystalline in different

synthesized conditions. All of the main peaks are between 2θ = 27.856 to 27.919 and 2θ = 46.292 to

46.431 that respectively are assigned to the planes of (112) and (204) at the tetragonal structure. It means that the structure is chalcopyrite (tetragonal) with space group I42d (JCPDS 27-0159). The results show the crystallinity has been completed in the duration of synthesis in both 2 and 4 hours cases. In some samples, their diffraction peaks also show lateral phase of copper sulfide. But this lateral phase is not as strong as the main structure. In the previous research Connor and coworkers [40] demonstrated that for synthesizing of Cu-In-S compound, the nucleation and growth of CuInS<sub>2</sub> start at the beginning of injection with Cu<sub>2</sub>S phase. Then result in biphasic Cu<sub>2</sub>S-CuInS<sub>2</sub> heterostructures. Finally, it could be converted to mono-phase nanoparticles at temperature above 250°C. Scheme 2 shows the arrangements of atomic planes and the positions of elemental space for both chalcocite (Cu<sub>2</sub>S) and chalcopyrite (CuInS<sub>2</sub>) structure. In fact, the Cu<sub>2</sub>S orthorhombic structure was converted to CuInS<sub>2</sub> body-centered tetragonal structure. The lattice parameters in the chalcopyrite structure of CuInS<sub>2</sub> (zincblende superlattice) are a=5.523Å, c=11.141Å and for chalcocite structure of Cu<sub>2</sub>S are a=11.881Å, b=27.323, c=13.491. Nearly similar crystal structure of orthorhombic and chalcopyrite results in low lattice distortion and energy barrier. Additionally, the fast diffusion of Cu<sup>+</sup> ions in the super ionic state of copper (I) sulfide together with enough synthesis time, result in an easily occurring conversion of Cu<sub>2</sub>S to CuInS<sub>2</sub> [41-43]. The temperature of 300°C was used for completing of reaction that was appropriate to convert copper sulfide to chalcopyrite structure whereas for less aggregation when reaction duration of synthesis was decreased from 4 hours to 2 hours, the copper sulfide phase was not completely converted to chalcopyrite structure and some lateral phase was remained.

The positions of the main peaks and planes are located at the 27.872 (112), 46.266 (220) and 55.043 (116) that proves the existence of chalcopyrite structure. The structural constants such as the lattice dimensions a, c, d and the tetragonal distortion ( $\eta=c/a$ ) are obtained as a=5.524Å, c=11.138Å d=3.198Å, and  $\eta=2.016$ , respectively. Figure 2 to 5 shows the TEM images of the CuInS<sub>2</sub> particles synthesized by different parameters. In order to analyze the effect of the anions solution temperature (including reducing agent) on the CuInS<sub>2</sub> particles, the solution of sulfide source was heated from 50°C to 150°C. Figure 2 shows by increasing the temperature of the solution including reducing agent (S<sup>2-</sup>), the particles size decreases but the size distribution becomes broader (CIS-WOA-M3). Carboxylic acid (OA) forms stable complexes with the precursors in comparison to OLA which are potentially useful as capping agent. Figure 3 shows the average particle diameters are from 10 to 200 nm for samples of CIS-WOA-M3 to CIS-WOA-M7 that is broad size distribution. When the ratio of OLA to OA is 3 to 1, a narrow size distribution is achieved but the particle size is not in the range of nanometer (CIS-WOA-M5).

To achieve this purpose (nanometer size and narrow distribution), the system condition was fixed by optimization of the parameters discussed. Thus, the temperature of the anions solution and the ratio of OLA to OA were set to 150°C and 3 to 1, respectively. Now the effect of the reaction duration and the temperature of the cations solution were investigated. Figure 4 demonstrates that the size and distribution of particles have not been improved by the decrease of reaction time while the increase of temperature of the cations solution at the moment of injection is really effective.

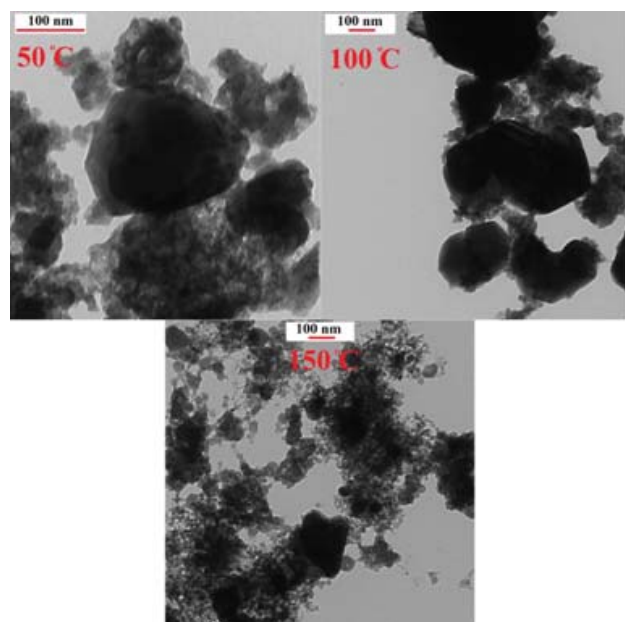


**Fig. 2.** Effect of anion solvent temperature in the injection instant.

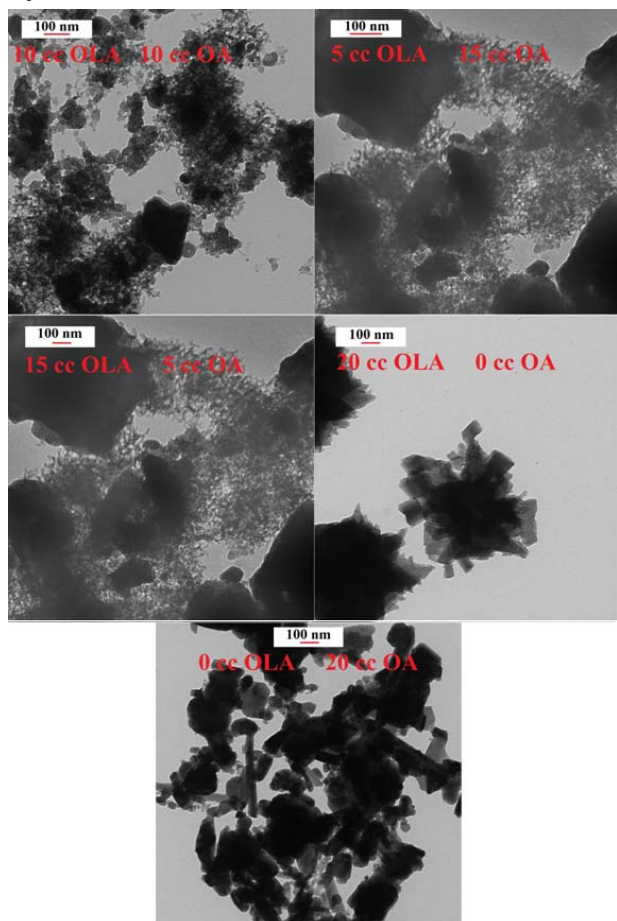


**Fig. 3.** Effect of solvent to capping agent ratio.

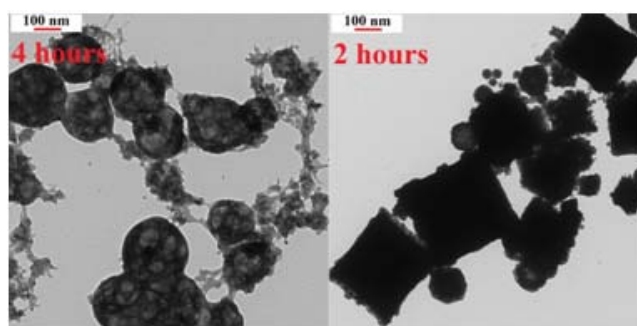


**Fig. 4.** Effect of duration of synthesis after injection.

These results reveal that the synthesis duration does not affect on the morphology. Therefore, the appropriate temperature of decomposition (in the injection instant) is really effective on the fast nucleation followed by the small growth and narrow size distribution of nuclei.

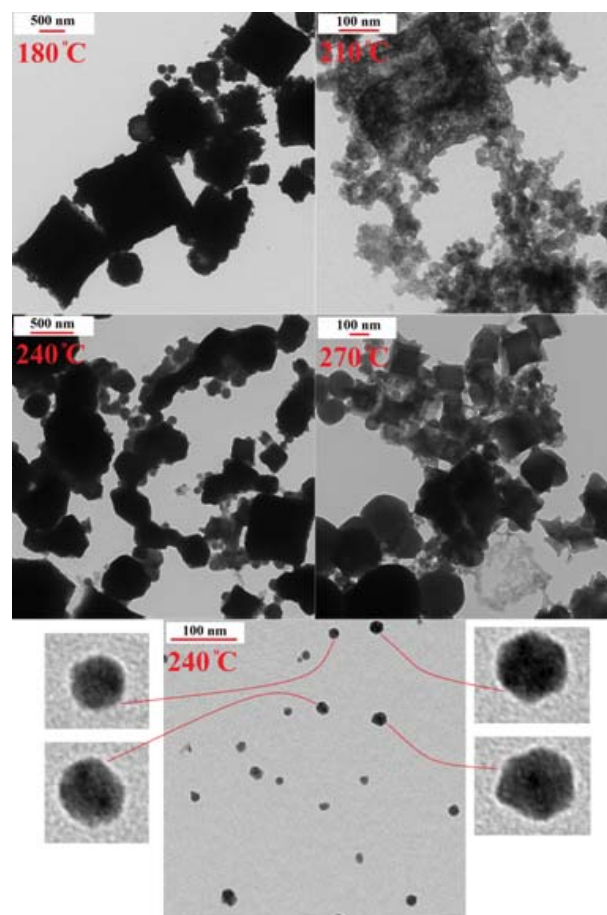


**Fig. 5.** Effect of temperature of metals solvent at the injection instant.

Figure 5, shows that 240°C is the best temperature to obtain nanometer size and narrow size distribution. The CuInS<sub>2</sub> of particles diameter is from 10 to 30 nm (CIS-WOA-M14) and the distribution is really improved in comparison with other samples. From the results it can be concluded that the optimized temperature for injection instant is 240°C as the smoke started producing after 200°C demonstrating occurrence of complex decomposition.

The plots of absorbance against wavelength in the UV and the visible region for the sample of CIS-WOA-M14, as optimized sample, are depicted in figure 6. The samples are dispersed in toluene with a mixture of 0.3 mg/ml under intense sonication of 15 min. The edge of absorbance starts

around the 840 nm but the absorbance shoulder is appeared at 810 nm. Additionally, the optical band gap of synthesized nanoparticles can be calculated by the extrapolation of the linear portion of the  $(\alpha h\nu)^2$  plots versus  $h\nu$  to  $\alpha = 0$  that shows the band gap is about 1.55 eV (CIS-WOA-M14). The photoluminescence (PL) spectra of the sample were measured at room temperature with excitation wavelengths of 650 nm. A broad PL band with maximum peak energy at 824 nm (1.51 eV) is observed showing the peak emission assignment to the band-band optical transition. In the PL spectra, the peak is broad due to the temperature of examine (room temperature) and the inhomogeneous broadening of peaks can be recognized as high concentration of defects [44].

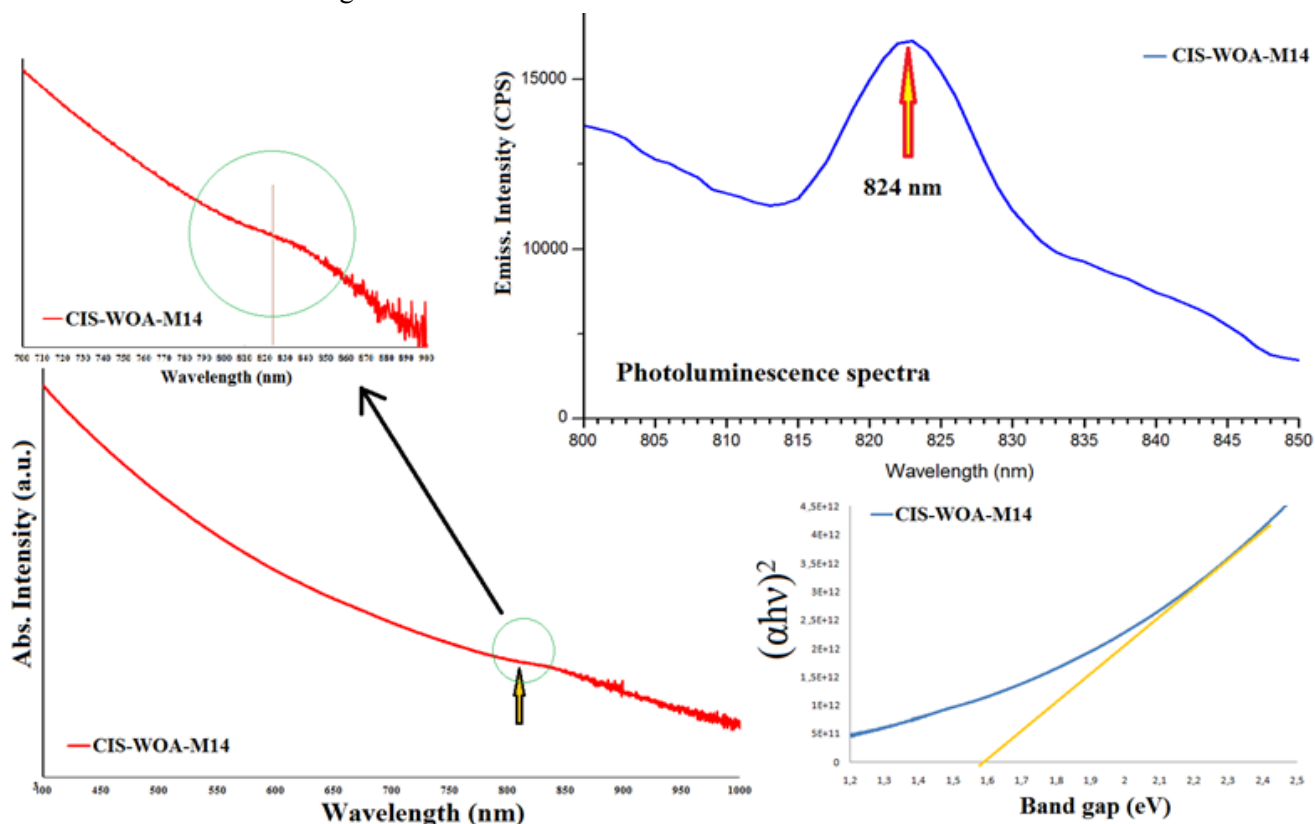


Fig. 6. Optical absorption and photoluminescence spectrum of CIS-WOA-M14 sample dispersed in toluene.

#### 4. Conclusion

In this research, we reported the preparation of the CuInS<sub>2</sub> chalcopyrite nanoparticles with an average size of 25 nm using the optimized hot injection method. It was concluded that the injection temperature plays a key role in the deformation of complex and follows formation of nuclei and controls the size and distribution. Although other research works [37-39] have reported the synthesis of wurtzite CuInS<sub>2</sub> Nanoparticles by hot injection, in this paper, the chalcopyrite structure was obtained. Additionally, no copper sulfide (Cu<sub>2-x</sub>S, x=1-2) lateral phase exists in the synthesized samples of this work as it has been confirmed in the most of wet synthesis methods.

#### Acknowledgment

The financial support of this work by the Research Council of Iran University of Science and Technology, and Engineering Research Institute are gratefully acknowledged.

#### References

- [1] W. Du, X. Qian, J. Yin, Q. Gong, *Chem. Eur. J.* 13 (2007) 8840-8846.
- [2] J. Tang, S. Hinds, S. O. Kelley, E. H. Sargent, *Chem. Mat.* 20 (2008) 6906-6910.
- [3] C. Jackson Stolle, M. G. Panthani, T. B. Harvey, V. A. Akhavan, B. A. Korgel, *Appl. Mater. Interfaces* 4 (2012) 2757-2761.
- [4] V. A. Akhavan, B. W. Goodfellow, M. G. Panthani, C. Steinhagen, T. B. Harvey, C. J. Stolle, B. A. Korgel, *J. Solid State Chem.* 189 (2012) 2-12.
- [5] X. Sheng, L. Wang, Y. Luo, D. Yang, *Nanoscale Research Letters* 6 (2007) 562.
- [6] T. L. Li, H. Teng, *J. Mater. Chem.* 20 (2007) 3656-3664.
- [7] Y. Vahidshad, R. Ghasemzadeh, A. Irajizad, M. Mirkazemi, A. Masoud, *J. Nanostruc.* 2 (2012) 369-377.
- [8] L. H. Tao, Z. J. Song, L. B. Feng, L. X. Juan, Y. X. Yu, J. H. Dong, Y. Fan, X. W. Dong, *Chin. Phys. Letter* 28 (2011) 057702.
- [9] F. B. Dejene, *Solar Energy Mater. & Solar Cells* 93 (2009) 577-582.
- [10] S. Siebentritt, *Solar Energy* 77 (2004) 767-775.
- [11] S. Jost, R. Schurr, A. Hölzing, F. Hergert, R. Hock, M. Purwins, J. Palm, *Thin Solid Films* 517 (2009) 2136-2139.
- [12] T. Koehler, S. Gledhill, A. Grimm, N. Allsop, C. Camus, A. Hänsel, W. Bohne, J. Röhrich, M. L. Steiner, C. H. Fischer, *Thin Solid Films* 517 (2009) 3332-3339.
- [13] R. Cayzac, F. Boulch, M. Bendahan, M. Pasquinelli, P. Knauth, *C. R. Chimie* 11 (2008) 1016-1022.
- [14] B. Asenjo, A. M. Chaparro, M. T. Gutiérrez, J. Herrero, *Thin Solid Films* 511 (2006) 117-120.
- [15] F. Cui, L. Wang, Z. Xi, Y. Sun, D. Yang, *J. Mater. Sci. Mater. Elect.* 20 (2009) 609-613.
- [16] M. Yousefi, M. Sabet, M. Salavati-Niasari, S. M. Hosseinpour-Mashkani, *J. Cluster Sci.* 23 (2012) 491-502.
- [17] V. A. Akhavan, B. W. Goodfellow, M. G. Panthani, C. Steinhagen, T. B. Harvey, C. J. Stolle, B. A. Korgel, *J. Solid State Chem.* 189 (2012) 2-12.
- [18] Z. Zhou, S. Yuan, J. Fan, Z. Hou, W. Zhou, Z. Du, S. Wu, *Nanoscale Research Letters* 7 (2012) 652.
- [19] J. Tang, S. Hinds, S. O. Kelley, E. H. Sargent, *Chem. Mater.* 20 (2008) 6906-6910.
- [20] R. Sharma, S. Shim, R. S. Mane, T. Ganesh, A. Ghule, G. Cai, D. H. Ham, S. K. Minb, W. Lee, S. H. Han, *Mater. Chem. Phys.* 116 (2009) 28-33.
- [21] W. Du, X. Qian, J. Yin, Q. Gong, *Chem. Eur. J.* 13 (2007) 8840-8846.

- [22] B. Koo, R. N. Patel, B. A. Korgel, J. A. Chem. Soc. 131 (2009) 3134-3135.
- [23] R. Swanepoel, J. Phys. E: Sci. Instrum. 16 (2007) 1214-1222.
- [24] J. C. W. Ho, S. K. Batabyal, S. S. Pramana, J. Lum, V. T. Pham, D. Li, Q. Xiong, A. I. Y. Tok, L. H. Wong, Mater. Express 2 (2012) 344-350.
- [25] X. Lu, Z. Zhuang, Q. Peng, Y. Li, Cryst. Eng. Comm. 13 (2011) 4039-4045.
- [26] W. C. Huang, C. H. Tseng, S. H. Chang, H. Y. Tuan, C. C. Chiang, L. M. Lyu, M. H. Huang, Langmuir 28 (2012) 8496-8501.
- [27] A. E. Rakhshani, J. Appl. Phys. 81 (1997) 7988-7993.
- [28] Y. Vahidshad, A. Irajizad, R. Ghasemzadeh, S. M. Mirkazemi, A. Masoud, Inter. J. Mod. Phys. B 26 (2012) 1250179-1250191.
- [29] S. Han, M. Kong, Y. Guo, M. Wang, Mater. Letters 63 (2009) 1192-1194.
- [30] S. T. Connor, C. M. Hsu, B. D. Weil, S. Aloni, Y. Cui, J. A. Chem. Soc. 131 (2009) 4962-4966.
- [31] N. Bao, X. Qiu, Y. H. A. Wang, Z. Zhou, X. Lu, C. A. Grimes, A. Gupta, Commun. 47 (2011) 9441-9443.
- [32] M. Kruszynska, H. Borchert, J. Parisi, J. K. Olesiak, J. A. Chem. Soc. 132 (2010) 15976-15986.
- [33] S. Lei, C. Wang, L. Liu, D. Guo, C. Wang, Q. Tang, B. Cheng, Y. Xiao, L. Zhou, Chem. Mater. 25 (2013) 25 2991-2997.
- [34] M. Deng, S. Shen, X. Wang, Y. Zhang, H. Xu, T. Zhang, Q. Wang, Cryst. Eng. Comm. 15 (2013) 6443-6447.
- [35] S. Mourdikoudis, L. M. L. Marzán, Chem. Mater. 25 (2013) 1465-1476.
- [36] B. L. Cushing, V. L. Kolesnichenko, C. J. O'Connor, Chem. Rev. 104 (2004) 3893-3946.
- [37] P. Shengjie, L. Y. Liang, C. F. Yi, L. I. Jing, Sci. China Chem. 55 (2012) 1236-1241.
- [38] Q. hang, J. J. Wang, Z. Jiang, Y. G. Guo, L. J. Wan, Z. Xie, L. Zheng, J. Mater. Chem. 22 (2012) 1765-1769.
- [39] Y. Luo, G. Chang, W. Lu, X. Sun, Coll. J. 72 (2010) 282-285.
- [40] S. T. Connor, C. M. Hsu, B. D. Weil, S. Aloni, Y. Cui, J. A. Chem. Soc. 131 (2009) 4962-4966.
- [41] D. Pan, L. An, Z. Sun, W. Hou, Y. Yang, Z. Yang, Y. Lu, J. A. Chem. Soc. 130 (2008) 5620-5621.
- [42] M. Kruszynska, H. Borchert, J. Parisi, J. K. Olesiak, J. A. Chem. Soc. 132 (2010) 15976-15986.
- [43] K. T. Yong, I. Roy, R. Hu, H. Ding, H. Cai, J. Zhu, X. Zhang, E. J. Bergeya, P. N. Prasad, Integr. Biol. 2 (2010) 121-129.
- [44] J. Van Gheluwe, J. Versluys, D. Poelman, J. Verschraegen, M. Burgelman, P. Clauws, Thin Solid Films 511-512 (2006) 304-308.